

## Epipelagic mesozooplankton communities in the northeastern Indian Ocean off Myanmar during the winter monsoon

Ping Du<sup>1, 2</sup>, Dingyong Zeng<sup>2</sup>, Feilong Lin<sup>2</sup>, Sanda Naing<sup>3</sup>, Zhibing Jiang<sup>1, 2</sup>, Jingjing Zhang<sup>1</sup>, Di Tian<sup>2</sup>, Qinghe Liu<sup>1</sup>, Yuanli Zhu<sup>1</sup>, Soe Moe Lwin<sup>4</sup>, Wenqi Ye<sup>1</sup>, Chenggang Liu<sup>1</sup>, Lu Shou<sup>1\*</sup>, Feng Zhou<sup>2</sup>

<sup>1</sup>Key Laboratory of Marine Ecosystem Dynamics, Second Institute of Oceanography, Ministry of Natural Resources, Hangzhou 310012, China

<sup>2</sup>State Key Laboratory of Satellite Ocean Environment Dynamics, Second Institute of Oceanography, Ministry of Natural Resources, Hangzhou 310012, China

<sup>3</sup>Port and Harbour Engineering Department, Myanmar Maritime University, Yangon 11293, Myanmar

<sup>4</sup>Geology Department, Dagon University, Yangon 11422, Myanmar

Received 9 May 2022; accepted 28 July 2022

© Chinese Society for Oceanography and Springer-Verlag GmbH Germany, part of Springer Nature 2023

### Abstract

The northern Andaman Sea off Myanmar is one of the relatively high productive regions in the Indian Ocean. The abundance, biomass and species composition of mesozooplankton and their relationships with environmental variables in the epipelagic zone (~200 m) were studied for the first time during the Sino-Myanmar joint cruise (February 2020). The mean abundance and biomass of mesozooplankton were  $(1\ 916.7 \pm 1\ 192.9)$  ind./m<sup>3</sup> and  $(17.8 \pm 7.9)$  mg/m<sup>3</sup>, respectively. A total of 213 species (taxa) were identified from all samples. The omnivorous Cyclopoida *Oncaea venusta* and *Oithona* spp. were the top two dominant taxa. Three mesozooplankton communities were determined via cluster analysis: the open ocean in the Andaman Sea and the Bay of Bengal (Group A), the transition zone across the Preparis Channel (Group B), and nearshore water off the Ayeyarwady Delta and along the Tanintharyi Coast (Group C). Variation partitioning analysis revealed that the interaction of physical and biological factors explained 98.8% of mesozooplankton community spatial variation, and redundancy analysis revealed that column mean chlorophyll *a* concentration (CMCHLA) was the most important explanatory variable (43.1%). The abundance and biomass were significantly higher in Group C, the same as CMCHLA and column mean temperature (CMT) and in contrast to salinity, and CMT was the dominant factor. Significant taxon spatial variations were controlled by CMCHLA, salinity and temperature. This study suggested that mesozooplankton spatial variation was mainly regulated by physical processes through their effects on CMCHLA. The physical processes were simultaneously affected by heat loss differences, freshwater influx, eddies and depth.

**Key words:** mesozooplankton, Myanmar, epipelagic zone, physical processes, water column mean chlorophyll *a*

**Citation:** Du Ping, Zeng Dingyong, Lin Feilong, Naing Sanda, Jiang Zhibing, Zhang Jingjing, Tian Di, Liu Qinghe, Zhu Yuanli, Lwin Soe Moe, Ye Wenqi, Liu Chenggang, Shou Lu, Zhou Feng. 2023. Epipelagic mesozooplankton communities in the northeastern Indian Ocean off Myanmar during the winter monsoon. *Acta Oceanologica Sinica*, 42(6): 57–69, doi: 10.1007/s13131-022-2090-5

### 1 Introduction

The Myanmar waters, located in the northern Andaman Sea, are part of the Bay of Bengal (BOB). The BOB is a semienclosed tropical basin located in the northeastern part of the Indian Ocean. The oceanographic characteristics of this basin exhibit seasonality due to semiannually reversing monsoon winds and currents, which are southwesterly during the summer (June–September) and northeasterly during the winter (November–February) (McCreary et al., 1993; Schott and McCreary, 2001; Shankar et al., 2002). The northern BOB has the widest shallow shelf region, extending more than 185 km to Bangladesh and approximately 65 km to Myanmar (Hossain et al., 2020). All major rivers of India (Krishna, Kaveri, Godavari, Mahanadi, Brahmaputra and Ganges), Bangladesh (Meghna) and Myanmar (Ayeyarwady, Thanlwin and Sittang) flow into the BOB. During the monsoon season, these rivers bring enormous quantities of

freshwater ( $1.6 \times 10^{12}$  m<sup>3</sup>/a) and suspended sediment ( $1.38 \times 10^9$  t/a) into the BOB (Subramanian, 1993). The freshwater inflow through rainfall and river influx exceeds evaporation and reduces the salinity in the upper layers of the basin, particularly in the northern region (Ittekkot et al., 1991; Prasanna Kumar et al., 2002).

The BOB is conventionally referred to as an oligotrophic and low biological production system. Suggested possible reasons for the low production include light limitations during monsoon periods and a low saline surface layer that inhibits the advection of nutrients from the subsurface (Gomes et al., 2000; Prasanna Kumar et al., 2002, 2010; Madhupratap et al., 2003; Madhu et al., 2006). However, there are two situations in which primary production is promoted in the BOB. First, episodic events such as eddies and gyres make the region locally productive in upper layers (Gomes et al., 2000; Prasanna Kumar et al., 2004; Nuncio and

Foundation item: The Scientific Research Fund of the Second Institute of Oceanography, Ministry of Natural Resources under contract No. JG2210; the Global Change and Air-Sea Interaction II Program under contract No. GASI-01-EIND-STwin; the National Natural Science Foundation of China under contract Nos 42176148 and 42176039.

\*Corresponding author, E-mail: [shoulu981@sio.org.cn](mailto:shoulu981@sio.org.cn)

Kumar, 2012; Jayalakshmi et al., 2015). Second, two higher productive zones ( $>2\ 000\ \text{mg}/(\text{m}^2\cdot\text{d})$ , in terms of C) exist in the upper layers of the northern coastal waters during the monsoon seasons, mainly in the Ganges-Brahmaputra-Meghna (GBM) Delta and Ayeyarwady Delta (Hossain et al., 2020).

Given the central role of zooplankton communities in food webs as consumers of primary production and prey for fish and organisms at higher trophic levels, changes in their communities have the potential to alter ecosystem structure (Fernández De Puellas and Molinero, 2008). Information on the zooplankton community of the BOB is limited. The northern Andaman Sea off Myanmar is one of the least studied regions. The study of zooplankton in this area has only been conducted during the International Indian Ocean Expedition (IIOE) (winter in the early 1960s) (Hossain et al., 2020) and First India–Myanmar Joint Oceanographic Expedition (April and May, 2002) (Jyothibabu et al., 2014). The biomass (displacement volume) and main groups of zooplankton were obtained during the IIOE (<https://www.st.nmfs.noaa.gov/copepod/>). Jyothibabu et al. (2014) showed how surface-layer zooplankton communities (only at  $\sim 2\ \text{m}$  depth) responded to environmental variables during the Spring Intermonsoon. However, studies integrating the zooplankton community and environmental variables in the epipelagic zone are lacking. The distribution of zooplankton is associated with hydrographic conditions, such as temperature, salinity, ocean currents and primary production in oligotrophic and mesotrophic oceans (Steinberg et al., 2012; Ashjian et al., 2017; Domínguez et al., 2017; Jagadeesan et al., 2017; Yuan and Pollard, 2018). Our research area is located in the northeastern BOB, which has different physicochemical characteristics (Jyothibabu et al., 2014), including those of coastal water off the Ayeyarwady Delta and Gulf of Mottama (shallow depth, lower salinity, higher temperatures, higher nutrient levels and suspended sediments), and open ocean water in the northern Andaman Sea and BOB (deep depth, higher salinity, lower temperatures, lower nutrients and suspended sediments). In addition, the region is under hypoxic stress. Based on the above characteristics, we hypothesize that there are spatial variations in the mesozooplankton community that are regulated by hydrography, dissolved oxygen (DO) and chlorophyll *a* (Chl *a*).

In this paper, we examined spatial variation in the mesozooplankton community off Myanmar during the winter monsoon and identified the dominant factors determining spatial variations in mesozooplankton biomass, abundance and community structure.

## 2 Materials and methods

### 2.1 Study area

The study area is located in the northeastern Indian Ocean, off the Ayeyarwady Delta and across the Preparis Channel, which is the northernmost channel connecting the Andaman Sea and the BOB (Fig. 1). The area includes shallow water ( $<100\ \text{m}$ ) in the Ayeyarwady continental shelf and deep water ( $>2\ 000\ \text{m}$ ) in the Andaman Sea and BOB. Ayeyarwady is the largest river in Myanmar, with an annual mean runoff of  $13\ 018\ \text{m}^3/\text{s}$  that enters the northern Andaman Sea through nine principal distributaries. The Ayeyarwady continental shelf width is approximately  $170\ \text{km}$  from the mouth of the Ayeyarwady River and increases to more than  $250\ \text{km}$  in the center of the Gulf of Mottama (Ramaswamy et al., 2008). A north–south trending  $120\ \text{km}$ -wide bathymetric depression is present toward the southern end of the continental shelf, and the Martaban Canyon lies within this depression (Rao et al., 2005). The Martaban Canyon cuts through the continental

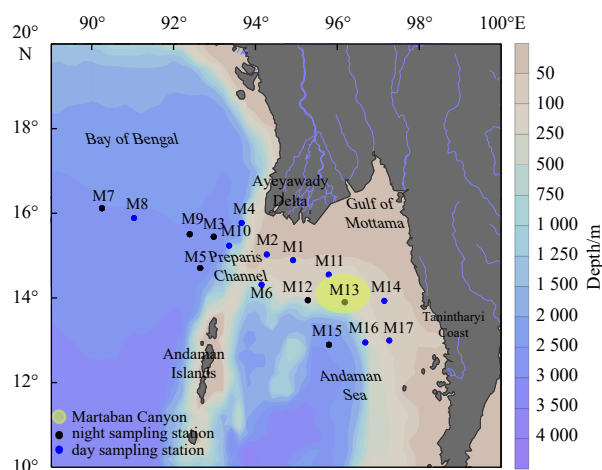


Fig. 1. Sampling stations in the northeastern Indian Ocean during February 2020.

shelf and the deep Andaman Sea (Ramaswamy et al., 2004). The northern Indian Ocean is characterized by the seasonally reversing Asian monsoon. During the summer monsoon, the Myanmar coastal areas are occasionally subjected to strong winds, while calm conditions typically prevail during the rest of the year (Ramaswamy et al., 2004). Freshwater and sediment discharge are also highly seasonal, with more than 80% of annual discharge occurring during the summer monsoon (Rodolfo, 1969). The large-scale spatiotemporal variation in nutrients, primary productivity and zooplankton in the BOB were simulated based on existing observation data (Hossain et al., 2020). The spatial distribution of nitrate in the upper 10 m indicated that the study area was devoid of nitrate ( $<0.1\ \mu\text{mol}/\text{L}$ ) during the winter monsoon; however, an improved situation was evident at  $0.1\text{--}0.3\ \mu\text{mol}/\text{L}$  during the summer monsoon. The phosphate concentration was  $0.2\text{--}0.3\ \mu\text{mol}/\text{L}$  during the winter monsoon, while a lower concentration ( $0.1\text{--}0.2\ \mu\text{mol}/\text{L}$ ) was observed during the summer monsoon. Regardless of season, the silicate concentration was high ( $3.0\text{--}3.7\ \mu\text{mol}/\text{L}$ ) in this area, possibly due to freshwater influx and residual flow. The most productive ( $>2\ 000\ \text{mg}/(\text{m}^2\cdot\text{d})$ , in terms of C) zone lies between  $15^\circ\text{--}17^\circ\text{N}$  and  $94^\circ\text{--}97^\circ\text{E}$ . There was a higher level of zooplankton biomass in this area ( $>40\ \text{mg}/\text{m}^3$ , in terms of C). The average net primary productivity level was slightly higher during the summer monsoon than during the winter monsoon (Hossain et al., 2020).

### 2.2 Sample collection

Seventeen stations were sampled in the northern Andaman Sea ( $12.89^\circ\text{--}16.15^\circ\text{N}$ ,  $90.24^\circ\text{--}97.27^\circ\text{E}$ ) onboard the R/V *Xiangy-anghong 6* from February 16 to 24, 2020 during the Sino-Myanmar joint cruise of the “Joint Advanced Marine and Ecological Studies in Exclusive Economic Zone of Myanmar”. The mesozooplankton samples were towed vertically from 200 m (or near the bottom for shallower stations) to the surface at a speed of approximately  $0.5\ \text{m}/\text{s}$  using WP2 plankton nets (200- $\mu\text{m}$  mesh,  $0.25\ \text{m}^2$  mouth size). The WP2 net was equipped with a calibrated flowmeter (HYDRO-BIOS, Germany) to determine the volume of water filtered. The day and night sampling stations were distinguished by local sunrise and sunset times (Table S1). One tow was collected at each station and was divided into two homogeneous subsamples using a Folsom plankton splitter (HYDRO-BIOS, Germany). One subsample was immediately preserved with a 5% buffered formalin-seawater solution for species identification and abundance counting; the other subsample was

filtered onto preweighed glass-fiber filters (Whatman GF/F filters, Whatman PLC., UK) and frozen at  $-80^{\circ}\text{C}$  for dry biomass measurements.

Temperature, salinity, and DO were measured using a Sea-Bird 911 CTD (Sea-Bird Electronics Inc., USA) and averaged into 1-m vertical intervals. The DO results measured by the CTD were corrected by the titration method for analysis. The seawater used for the Chl *a* measurements was collected from 5 to 7 layers (2 m, 30 m, 50 m, 75 m, 100 m, 150 m and 200 m or bottom) in the upper 200-m column at each station. One liter of seawater was filtered through GF/F filters and then extracted with 90% acetone in the dark at  $-20^{\circ}\text{C}$  for 24 h, and finally, Chl *a* was measured using a Turner Designs fluorometer (Turner Designs Inc., USA). For the size-fractionated Chl *a* from micro- ( $>20\ \mu\text{m}$ ), nano- (2–20  $\mu\text{m}$ ), and pico- (0.7–2  $\mu\text{m}$ ) phytoplankton, one liter of seawater was sequentially filtered through polycarbonate membranes with pore sizes of 20  $\mu\text{m}$  and 2  $\mu\text{m}$  (Millipore Inc., USA) and GF/F filters with a pore size of 0.7  $\mu\text{m}$  (Whatman PLC., UK). The integrated Chl *a* concentration in the water column from 200 m or the bottom to the surface was calculated using the trapezoidal rule. The mixed layer depth (MLD) was taken as the depth at which the sigma-t values were more than 0.2 greater than the surface value (Prasanna Kumar et al., 2004).

### 2.3 Mesozooplankton community analysis

For the microscopy analysis, all the mesozooplankton species were divided using a Folsom plankton splitter and counted in aliquots ranging from 1/2 to 1/8 of the total volume (according to the numerical density of the individuals). Subsamples consisting of approximately 500 specimens were counted using a dissecting microscope (ZEISS Stemi 2000-c, Germany). During the mesozooplankton identification process, all adult Copepoda, Cnidaria, Ctenophora, Chaetognatha, and Amphipoda in Malacostraca, Cladocera, and Ostracoda were identified to the species or genus level when the key parts for identification were destroyed or the earlier life stages could not be resolved to species. The copepodids of the genera *Clausocalanus* and *Paracalanus* were treated as *Clausocalanus/Paracalanus* larva because of the difficulty of genus-level identification. All Polychaeta and Mollusca were identified to the genus level. All Appendicularia and Thaliaceae were identified to the family level. Mysida, Euphausiacea, Decapoda and Cumacea, which occurred at a low abundance, were identified to the order level. Protozoa were identified to the phylum level. The planktonic larvae were grouped at the taxa level.

The mesozooplankton abundance ( $\text{ind.}/\text{m}^3$ ) is equal to that the number of individuals divided by the multiplication of splitting ratio and net volume. The mesozooplankton samples for the dry weight measurements were rinsed with distilled water to remove salts and then dried in an oven at  $60^{\circ}\text{C}$  for 72 h. The dry samples were measured using an analytical balance (Sartorius BSA124S, Germany) with a precision of 0.1 mg. Biomass is equal to that the dry weight divided by the multiplication of splitting ratio and net volume. The dominant species were defined as those with an average relative abundance of more than 1% in at least one group.

### 2.4 Statistical analysis

Hierarchical cluster analysis based on the Bray–Curtis index was performed to determine mesozooplankton community similarities after the data were  $\ln(X+1)$  transformed using PRIMER 6.0 (Plymouth, UK). One-way analysis of similarities (ANOSIM) was conducted to test the statistical significance of differences in

mesozooplankton communities between groups produced by cluster analysis and between day and night sampling stations by PRIMER 6.0. Interactive-forward-selection redundancy analyses (RDAs) were performed to explore the relationships between the mesozooplankton taxonomic composition and the environmental variables. These variables included physical factors (depth, MLD, sea surface temperature (SST), sea surface salinity (SSS), column mean temperature (CMT) and column mean salinity (CMS)), chemical factors (sea surface DO (SDO) and column mean DO (CMDO)), and biological factors (sea surface Chl *a* (SCHLA) and column mean Chl *a* (CMCHLA) concentrations) (Table S2). “Var-part-3groups-simple-effects-tested-FS” variation partitioning analysis (VPA) was performed to explore the individual and combined contributions of physical, chemical, and biological factors to mesozooplankton community spatial variation. RDA and VPA were performed using CANOCO 5.0 (Šmilauer and Lepš, 2014). The statistical significance of differences in the dry biomass, abundance and relative abundance (%) of the taxa and the dominant species of mesozooplankton between the groups produced by cluster analysis was analyzed using the Kruskal–Wallis test. Spearman correlation analysis and multiple linear regression (MLR) analysis (backward) were used to model the relationship between the explanatory variables and the biomass or abundance of mesozooplankton. The Spearman correlation analyses, Kruskal–Wallis test and MLR were performed using SPSS 20.0. The significance of the differences and correlations above was evaluated by means of the adjusted *p* value, with a significance level of  $p < 0.05$ .

## 3 Results

### 3.1 Environmental variables

The depth of the study area ranged from 52 m to 2 801 m and increased from the Myanmar continental shelf to the Andaman Sea and BOB (Fig. 2). The MLD ranged from 8 m to 47 m (Fig. 2). Temperature and DO concentrations decreased along the depth profile, while salinity increased along the depth profile; the DO concentration decreased rapidly from 6 mg/L to 2 mg/L through the oxycline, among which the shallowest was 10–19 m and the deepest was 68–84 m (Fig. 3).

During the sampling period, SST ranged from  $25.4^{\circ}\text{C}$  to  $28.5^{\circ}\text{C}$  and exhibited a tendency to increase from northwest to southeast (Fig. 4a); SSS ranged from 30.6 to 32.6 with lower salinity near the Ayeyarwady Delta (Fig. 4b). Additionally, the SDO ranged from 6.16 mg/L to 6.57 mg/L, with a tendency to decrease from west to east (Fig. 4c). The SCHLA concentration ranged from 0.27  $\mu\text{g}/\text{L}$  to 1.35  $\mu\text{g}/\text{L}$ , with the highest values occurring around the Ayeyarwady Delta and the second highest values oc-

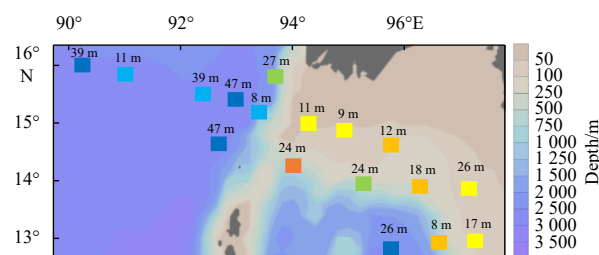
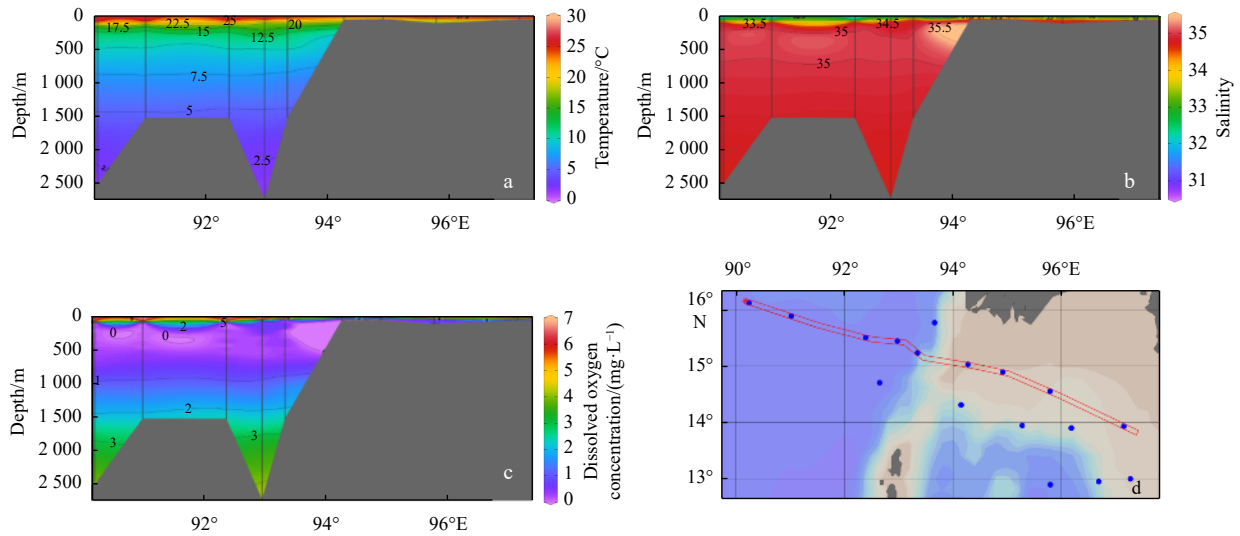
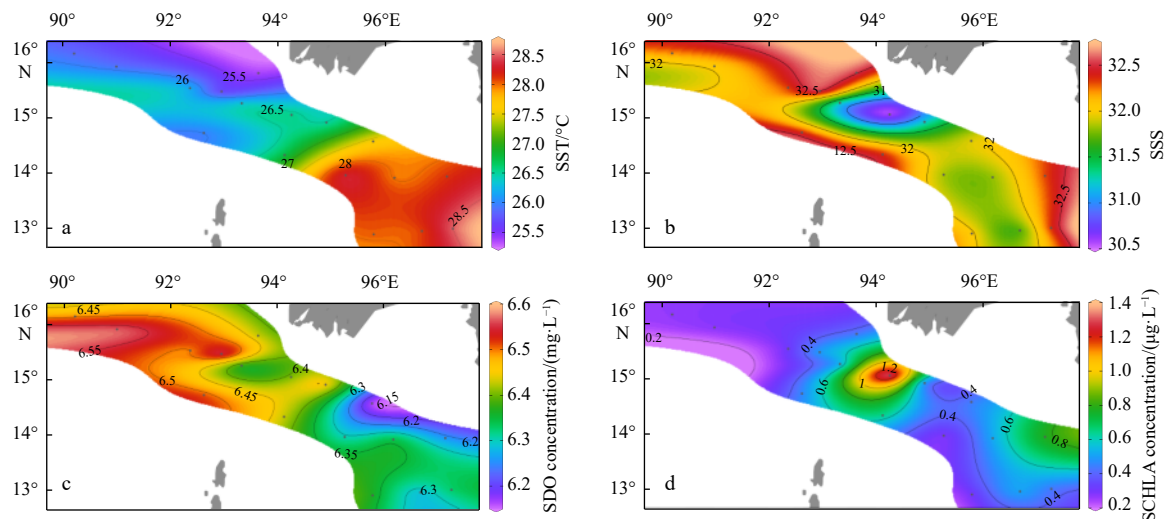


Fig. 2. Water depth and mixed layer depth (MLD) measured during the sampling period. The different colors of squares indicate water depths: yellow: 52–79 m, orange: 112–137 m, dark orange: 295 m, green: 639–766 m, blue: 1 517–1 523 m, dark blue: 2 431–2 801 m. Numbers above the square indicate MLDs.



**Fig. 3.** Vertical profiles of temperature (a), salinity (b) and dissolved oxygen concentration (c) of the selected section (d).



**Fig. 4.** Surface values of temperature (a), salinity (b), dissolved oxygen concentration (c), and chlorophyll *a* concentration (d). SST: sea surface temperature; SSS: sea surface salinity; SDO: surface dissolved oxygen; SCHLA: surface chlorophyll *a*.

curing along the Tanintharyi Coast (Fig. 4d).

Referring to the mean value in the column of mesozooplankton towed depth, CMT ranged from 19.4°C to 26.0°C, the highest values were along the Tanintharyi Coast, and the second highest values were around the Ayeyarwady Delta (Fig. 5a). CMS ranged from 33.2 to 34.3, the spatial trend was the opposite to that of temperature, the lowest values were along the Tanintharyi Coast, and the second lowest values were around the Ayeyarwady Delta (Fig. 5b). CMDO ranged from 1.59 mg/L to 4.41 mg/L; the highest values were along the Tanintharyi Coast, and the lowest values were near the channel connecting the Andaman Sea and BOB (Fig. 5c). The CMCHLA ranged from 0.22 µg/L to 1.02 µg/L, and the spatial trend was the opposite to that of salinity and consistent with that of temperature. The highest values were along the Tanintharyi Coast, and the second highest values were around the Ayeyarwady Delta (Fig. 5d).

### 3.2 Mesozooplankton community

#### 3.2.1 Whole area

Overall, the dry biomass of mesozooplankton ranged from

3.7 mg/m<sup>3</sup> to 30.7 mg/m<sup>3</sup> (mean (17.8±7.9) mg/m<sup>3</sup>), and the total abundance ranged from 337.5 ind./m<sup>3</sup> to 4 454.0 ind./m<sup>3</sup> (mean (1 916.7±1 192.9) ind./m<sup>3</sup>). A total of 213 species or taxa (including 17 categories of planktonic larvae) belonging to 12 taxonomic groups were identified from all samples. Of these, 174 adult species were identified. The mesozooplankton taxonomic compositions were dominated by the subclass Copepoda (relative abundance 72.8%–91.9%, mean 82.5%±5.9%), followed by the sub-phylum Tunicata (class Appendicularia 2.1%–18.3%, mean 8.3%±4.3%; class Thaliacea 0–2.2%, mean 0.6%±0.6%), planktonic larva (0.9%–5.7%, mean 2.5%±1.4%), subclass Ostracoda (0–8.3%, mean 2.3%±2.2%), phylum Chaetognatha (0–3.2%, mean 1.4%±0.9%) and phylum Cnidaria (0–1.9%, mean 0.8%±0.7%), while the mean relative abundances of the phylum Protozoa, phylum Ctenophora, phylum Mollusca, phylum Polychaeta, subclass Malacostraca, and subclass Cladocera were all lower than 0.5%. The top 10 dominant species included nine copepods (*Oncaea venusta*, *Oithona* spp., *Paracalanus aculeatus*, *Clausocalanus farrani*, *Clausocalanus furcatus*, *Subeucalanus subtenius*, *Acrocalanus gibber*, *Farranula gibbula*, and *Triconia conifera*) and one Appendicularia genus (*Oikopleura* spp.).

3.2.2 Spatial variations in the mesozooplankton community

The mesozooplankton community was divided into 3 groups (A: open ocean, B: transition zone, C: nearshore water) at 50% similarity by cluster analysis based on taxonomic compositions; furthermore, Group B was divided into 2 subgroups (B-1 and B-2) at 60% similarity, while Group C was divided into 3 subgroups (C-1, C-2 and C-3) at 61% similarity (Fig. 6). One-way ANOSIM showed that the differences among the three groups were significant (Global  $R = 0.656$ ,  $p < 0.001$ ), and pairwise tests showed that the differences between groups were all significant ( $p_{AB} = 0.022$ ,  $p_{AC} = 0.028$ ,  $p_{BC} = 0.001$ ). Additionally, the difference between the 2 subgroups in Group B was significant ( $p = 0.029$ ), while the differences between the 3 subgroups in Group C were not significant ( $p_{C12} = 0.100$ ,  $p_{C13} = 0.333$ ,  $p_{C23} = 0.100$ ). To exclude the influence of day-night sampling on the mesozooplankton community, ANOSIM was used to test the mesozooplankton community difference between stations sampled during the night and during the day, and the results showed that the difference was not significant ( $p = 0.118$ ).

3.2.3 Spatial variations in abundance and biomass

The spatial variations in the abundance and dry biomass of mesozooplankton were consistent, and higher values were detected around the Ayeyarwady Delta and along the Tanintharyi Coast (Fig. 7). Based on the Kruskal–Wallis test, the abundance and biomass of Group C were both significantly higher than those of the remaining two groups (abundance: adjusted  $p_{AC} = 0.007$ , adjusted  $p_{BC} = 0.017$ ; biomass: adjusted  $p_{AC} = 0.006$ , adjusted  $p_{BC} = 0.012$ ), but the differences in the abundance and biomass between Group A and Group B were not significant. The differences in abundance and biomass between subgroups were not significant (Table 1).

3.2.4 Spatial variations in taxonomic groups and dominant species

The order Mormonilloida in the subclass Copepoda, subclass Ostracoda, class Thaliaceae and phylum Chaetognatha exhibited significant spatial differences among groups. The relative abundances of the four taxonomic groups were significantly higher in

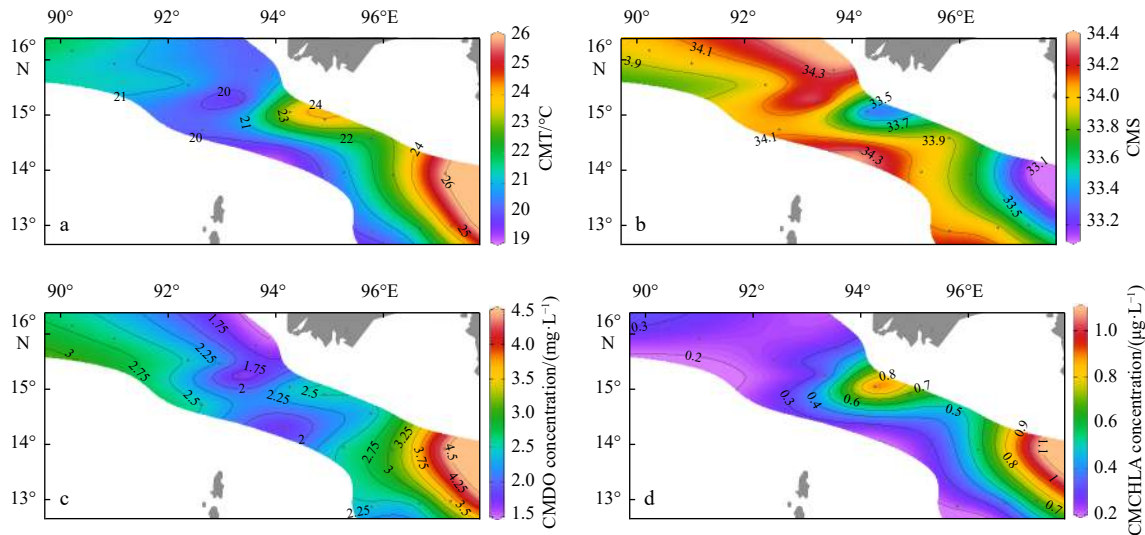


Fig. 5. Column mean values of temperature (a), salinity (b), dissolved oxygen concentration (c), and chlorophyll *a* concentration (d) from 200 m (or the bottom) to the surface. CMT: column mean temperature; CMS: column mean salinity; CMDO: column mean dissolved oxygen; CMCHLA: column mean chlorophyll *a*.

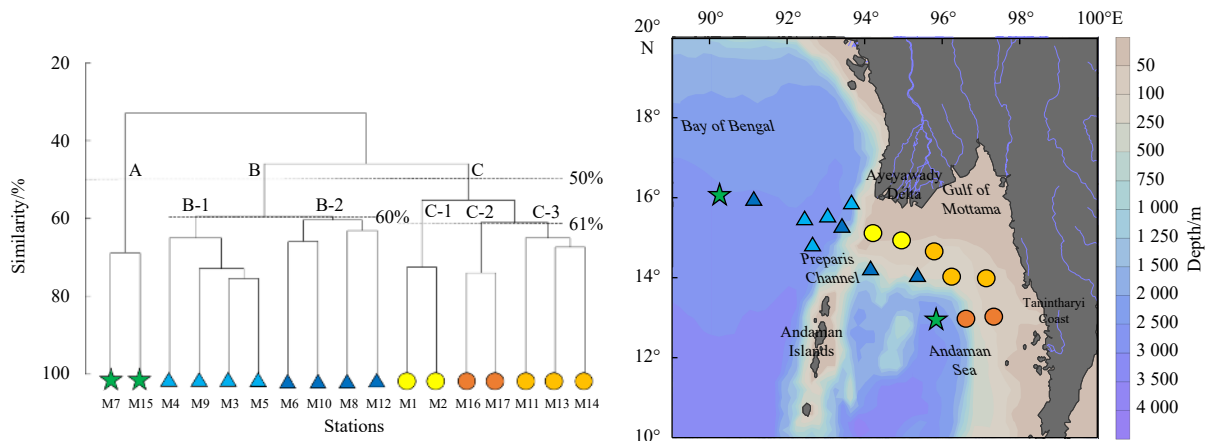


Fig. 6. Mesozooplankton community clusters according to taxonomic abundance datasets. Three groups (A: open ocean, B: transition zone, C: nearshore water) were divided at 50% similarity; Group B was divided into two subgroups (B-1 and B-2) at 60% similarity, while Group C was divided into three subgroups (C-1, C-2 and C-3) at 61% similarity. Green stars indicate Group A; light and dark blue triangles indicate Groups B-1 and B-2, respectively; yellow, orange and light orange circles indicate Groups C-1, C-2 and C-3, respectively.

Group B than in Group C (Table 2). Significant spatial differences among groups were also detected in the six dominant species. The relative abundances of *Clausocalanus farrani* and *Euchaeta concinna* (Copepoda: Calanoida) were significantly higher in Group C than in Group B; those of *Mormonilla phasma* (Copepoda: Mormonilloida) and *Cypridina dentata* (Ostracoda) were significantly higher in Group B than in Group C; those of *Calocalanus plumulosus* (Copepoda: Calanoida) were significantly higher in Group A than in Group C; and those of *Pleuromamma robusta* (Copepoda: Calanoida) were significantly

higher in Group A than in Groups B and C (Table 3).

### 3.3 Relationship between the mesozooplankton community and the environmental variables

#### 3.3.1 Spatial variations in environmental variables

According to the Kruskal–Wallis test for the ten environmental variables, there were significant spatial variations in depth, CMT, CMCHLA and CMS. Depth and CMS were both significantly higher in Groups A and B than in Group C. CMT and

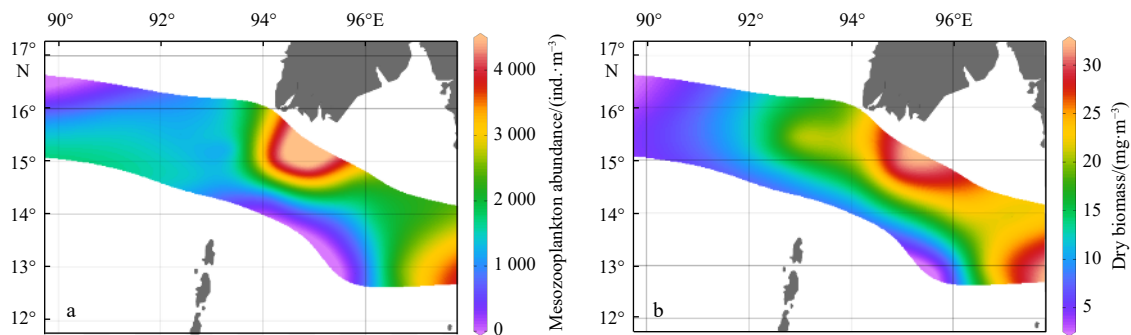


Fig. 7. Spatial variations in mesozooplankton abundance (a) and dry biomass (b) in towed water column (200 m or from the bottom to the surface for shallower stations).

Table 1. Spatial variations in mesozooplankton abundance (ind./m<sup>3</sup>) and dry biomass (mg/m<sup>3</sup>)

Group	Subgroup	Abundance in subgroup	Dry biomass in subgroup	Abundance in groups	Dry biomass in groups
A	–	–	–	394.7±80.9 <sup>b</sup>	4.0±0.4 <sup>b</sup>
B	B-1	1 519.8±268.7	16.3±4.7	1 265.7±343.8 <sup>b</sup>	15.2±4.7 <sup>b</sup>
	B-2	1 011.6±177.2	14.2±5.2		
C	C-1	4 332.7±171.6	26.3±6.2	2 958.5±1 030.3 <sup>a</sup>	24.8±3.7 <sup>a</sup>
	C-2	2 116.0±298.0	23.6±3.3		
	C-3	2 848.1±481.1	25.0±3.9		

Note: Different lowercase letters (a, b) in the same index indicate significant differences among groups ( $p < 0.05$ ). – represents no data.

Table 2. Spatial variations in the relative abundances (%) of the mesozooplankton taxa

Taxonomic groups	Order	Differences in Order			Differences in Taxonomic groups		
		Group A	Group B	Group C	Group A	Group B	Group C
Subclass Copepoda	Calanoida	38.2±0.6	37.3±8.1	44.7±4.7	81.4±7.6	79.9±5.0	85.9±5.7
	Cyclopoida	40.2±5.9	39.0±6.5	40.8±8.0			
	Harpacticoida	0.4±0.1	0.5±0.3	0.3±0.3			
	>Mormonilloida	2.6±1.2 <sup>ab</sup>	3.2±2.2 <sup>a</sup>	0.1±0.3 <sup>b</sup>			
Subclass Malacostraca	Amphipoda	0.1±0.1	0.2±0.2	0.0±0.1	0.3±0.4	0.6±0.4	0.2±0.3
	Mysida	0.0±0.0	0.0±0.0	0.0±0.0			
	Euphausiacea	0.2±0.3	0.4±0.3	0.1±0.1			
	Decapoda	0.0±0.0	0.0±0.0	0.0±0.1			
	Cumacea	0.0±0.0	0.0±0.0	0.0±0.0			
Subclass Phyllopoda	Cladocera	–	–	–	0.2±0.3	0.1±0.2	0.0±0.0
Subclass Ostracoda	–	–	–	2.1±0.6 <sup>ab</sup>	3.6±2.6 <sup>a</sup>	0.9±0.6 <sup>b</sup>	
Class Appendicularia	–	–	–	8.7±4.7	8.9±3.7	7.6±5.2	
Class Thaliacea	–	–	–	0.5±0.0 <sup>ab</sup>	1.0±0.7 <sup>a</sup>	0.1±0.2 <sup>b</sup>	
Class Polychaeta	–	–	–	0.3±0.0	0.2±0.3	0.2±0.3	
Phylum Chaetognatha	–	–	–	1.7±0.8 <sup>ab</sup>	1.9±0.7 <sup>a</sup>	0.8±0.6 <sup>b</sup>	
Phylum Cnidaria	–	–	–	0.4±0.1	1.2±0.6	0.4±0.6	
Phylum Ctenophora	–	–	–	0.0±0.0	0.0±0.0	0.0±0.0	
Phylum Mollusca	–	–	–	0.8±0.1	0.3±0.2	0.6±0.7	
Phylum Protozoa	–	–	–	0.5±0.5	0.2±0.2	0.4±0.3	

Note: Different lowercase letters (a, b) in the same index indicate significant differences among groups ( $p < 0.05$ ). – represents these taxonomic groups are not subdivided by order.

CMCHLA were both significantly higher in Group C than in Group B (Table 4). The proportion of micro- and nano-Chl *a* was higher in Group C than in Groups A and B, while the proportion of pico-Chl *a* was lower in Group C than in Groups A and B; however, the Kruskal–Wallis test was not performed for size-fractionated Chl *a* because it was measured only at representative stations (M7 in Group A; M9 in Group B; M1, M2, M13, and M14 in Group C) (Table 4).

### 3.3.2 Mesozooplankton community

The interactive-forward-selection RDA showed that the ten environmental variables together could account for 85.9% of the total mesozooplankton community variation (adjusted explained variation after Bonferroni correction was 62.5%); therein, the physical and biological factors accounted for 25.2% and 45.7%, respectively. The influences of CMCHLA, CMT, CMDO and CMS were significant, and the four variables together ac-

**Table 3.** Spatial variations in the relative abundances (%) of the dominant species

Taxa	Dominant species	Group A	Group B	Group C
Copepoda	<i>Oncaea venusta</i>	23.6±4.2	19.9±6.5	22.9±6.2
Copepoda	<i>Oithona</i> spp.	10.6±1.2	12.0±3.0	13.9±5.0
Copepoda	<i>Paracalanus aculeatus</i>	10.8±2.6	7.8±3.0	13.8±6.9
Appendicularia	<i>Oikopleura</i> spp.	7.7±4.5	8.4±3.5	7.5±5.2
Copepoda	<i>Clausocalanus farrani</i>	6.0±0.3 <sup>ab</sup>	3.0±1.6 <sup>b</sup>	6.9±3.0 <sup>a</sup>
Copepoda	<i>Subeucalanus subtenuis</i>	0.7±0.6	2.3±2.0	3.9±2.9
Copepoda	<i>Clausocalanus furcatus</i>	2.9±1.7	5.2±2.5	2.8±2.3
Copepoda	<i>Euchaeta</i> larva	1.7±0.0	1.6±0.7	2.7±2.4
Copepoda	<i>Clausocalanus/Paracalanus</i> larva	1.4±0.4	2.5±2.0	2.6±2.6
Copepoda	<i>Neocalanus</i> larva	2.8±1.0	2.3±1.4	2.5±1.4
Copepoda	<i>Acrocalanus gibber</i>	0.9±0.3	1.8±1.0	1.9±1.2
Copepoda	<i>Farranula gibbula</i>	2.8±0.1	1.7±1.2	1.4±0.9
Copepoda	<i>Triconia conifera</i>	0.7±0.6	2.2±1.3	1.0±0.6
Copepoda	<i>Euchaeta concinna</i>	0.7±0.6 <sup>ab</sup>	0.2±0.2 <sup>b</sup>	1.0±0.9 <sup>a</sup>
Copepoda	<i>Canthocalanus pauper</i>	0.5±0.2	1.2±0.7	1.0±0.8
Copepoda	<i>Mormonilla phasma</i>	2.6±1.2 <sup>ab</sup>	3.2±2.2 <sup>a</sup>	0.1±0.3 <sup>b</sup>
Ostracoda	<i>Cypridina dentata</i>	0.1±0.2 <sup>ab</sup>	1.7±1.9 <sup>a</sup>	0.2±0.3 <sup>b</sup>
Copepoda	<i>Temora turbinata</i>	0.3±0.4	1.5±1.8	0.6±1.6
Copepoda	<i>Scolecithricella nicobarica</i>	0.7±0.6	1.3±0.8	0.7±0.5
Ostracoda	<i>Euconchoecia aculeata</i>	0.9±0.1	1.0±0.7	0.5±0.5
Copepoda	Corycaeidae larva	0.2±0.2	1.0±0.7	0.5±0.7
Copepoda	<i>Calocalanus plumulosus</i>	1.5±0.9 <sup>a</sup>	0.3±0.4 <sup>ab</sup>	0.1±0.2 <sup>b</sup>
Planktonic larva	Copepoda nauplius larva	1.3±0.6	0.4±0.4	0.9±0.6
Copepoda	<i>Pleuromamma robusta</i>	1.0±1.0 <sup>a</sup>	0.3±0.1 <sup>b</sup>	0.1±0.1 <sup>b</sup>
Appendicularia	Fritillariidae spp.	1.0±0.2	0.5±0.5	0.1±0.1
Chaetognatha	<i>Serratosagitta pacifica</i>	1.0±0.6	0.4±0.3	0.5±0.5

Note: Dominant species were defined as having a relative abundance of greater than 1% in at least one group. Different lowercase letters (a, b) in the same index indicate significant differences among groups ( $p < 0.05$ ).

**Table 4.** Spatial variations in the environmental variables by the Kruskal–Wallis test

Environmental variables	Group A	Group B	Group C
Depth/m	2 468.5±53.0 <sup>a</sup>	1 473.6±920.3 <sup>a</sup>	89.1±35.0 <sup>b</sup>
MLD/m	32.5±9.2	28.4±14.9	14.4±6.3
SST/°C	27.0±1.5	26.3±0.9	27.6±0.8
SSS	32.1±0.1	32.2±0.5	31.7±0.6
SDO concentration/(mg·L <sup>-1</sup> )	6.4±0.1	6.5±0.1	6.3±0.1
SCHLA concentration/(µg·L <sup>-1</sup> )	0.3±0.0	0.4±0.1	0.6±0.3
CMT/°C	21.0±0.9 <sup>ab</sup>	20.3±0.6 <sup>b</sup>	23.6±1.4 <sup>a</sup>
CMS	34.0±0.1 <sup>a</sup>	34.1±0.2 <sup>a</sup>	33.6±0.3 <sup>b</sup>
CMDO concentration/(mg·L <sup>-1</sup> )	2.6±0.2	2.2±0.4	3.0±0.8
CMCHLA concentration/(µg·L <sup>-1</sup> )	0.3±0.1 <sup>ab</sup>	0.3±0.0 <sup>b</sup>	0.7±0.2 <sup>a</sup>
Micro SCHLA/%	7.1	8.5	20.8±8.0
Nano SCHLA/%	15.9	13.7	19.6±5.5
Pico SCHLA/%	77.0	77.7	59.6±11.6

Note: Different lowercase letters (a, b) in the same index indicate significant differences between groups ( $p < 0.05$ ). Size-fractionated chlorophyll *a* concentrations were measured only at representative stations (M7 in Group A; M9 in Group B; M1, M2, M13, M14 in Group C). A Kruskal–Wallis test was not performed for size-fractionated Chl *a*. MLD: mixed layer depth; SST: sea surface temperature; SSS: sea surface salinity; SDO: surface dissolved oxygen; SCHLA: surface chlorophyll *a*; CMT: column mean temperature; CMS: column mean salinity; CMDO: column mean dissolved oxygen; CMCHLA: column mean chlorophyll *a*. Micro SCHLA, Nano SCHLA and Pico SCHLA represent proportions of micro- (>20 µm), nano- (2–20 µm), and pico- (0.7–2 µm) surface chlorophyll *a* concentration to total surface chlorophyll *a* concentration, respectively.

counted for 75.0% of the total mesozooplankton community variation (Fig. 8, Table 5). Furthermore, VPA results showed that the interaction of physical and biological factors was the most important explanatory variable, potentially accounting for 98.8% of mesozooplankton community spatial variation (f in Fig. 9, Table S3).

### 3.3.3 Biomass and abundance

Both the biomass and abundance of mesozooplankton were positively correlated with CMCHLA and CMT, but negatively significantly correlated with depth and CMS. In addition, biomass was significantly negatively correlated with MLD and SDO.

The linear regression analysis models of mesozooplankton biomass and abundance with the ten environmental variables

were biomass=1.28CMT-0.86CMDO-3.37 ( $p=0.003$ ) and abundance=1.54CMT-1.01CMDO-7.06 ( $p=0.000$ ), respectively, suggesting that the biomass and abundance of mesozooplankton were both mainly affected by CMT and CMDO. However, Spearman correlation analyses showed that the coefficients of correlation between the biomass and abundance of mesozooplankton and CMDO were not significant (Table S4). Therefore, CMT was the main factor affecting the spatial variation in mesozooplankton biomass and abundance.

### 3.3.4 Taxonomic groups and dominant species

To screen the environmental variables controlling the spatial variations in mesozooplankton taxa, the four taxonomic groups and six dominant species with significant spatial differences were selected for interactive-forward-selection RDA with the ten environmental variables. The results showed that the ten environmental variables together accounted for 78.5% of the spatial variation in taxa (adjusted explained variation after Bonferroni correction was 42.7%). Therein, the influences of CMCHLA, CMS and SST were significant, and the three variables together accounted for 49.1% of the mesozooplankton taxa spatial variation (Fig. 10, Table 5). *Clausocalanus farrani* and *Euchaeta concinna* (Copepoda: Calanoida) preferred areas with higher temperatures and Chl *a* concentrations. Ostracoda (*Cypridina dentata*), Thaliaceae, Chaetognatha, Mormonilloida (*Mormonilla phasma*), *Calocalanus plumulosus* and *Pleuromamma robusta* preferred the areas with deeper water, higher salinity, and lower temperature, CMDO, and Chl *a* concentrations.

## 4 Discussion

### 4.1 Mesozooplankton composition and ecosystem characteristics

A total of 213 species (taxa) were identified in this study, of which 174 adult species were identified. Copepods were the predominant taxonomic group (relative abundance 72.8%–91.9%; containing 96 species of adult copepods). Importantly, the WP2 net could not collect macrozooplankton efficiently because of their active avoidance of the sampler (Skjoldal et al., 2013), so macrozooplankton, such as euphausiid and fish larvae, were underestimated in this study. The total species number found in our study was higher than those reported for other Indian waters and similar to those found in the open water of the BOB and Pacific (Table 6). That is, the number of mesozooplankton species in this area is relatively high in Indo-Pacific waters. This was mainly found due to the inclusion of both nearshore and offshore stations in this study. It was evident that species composition

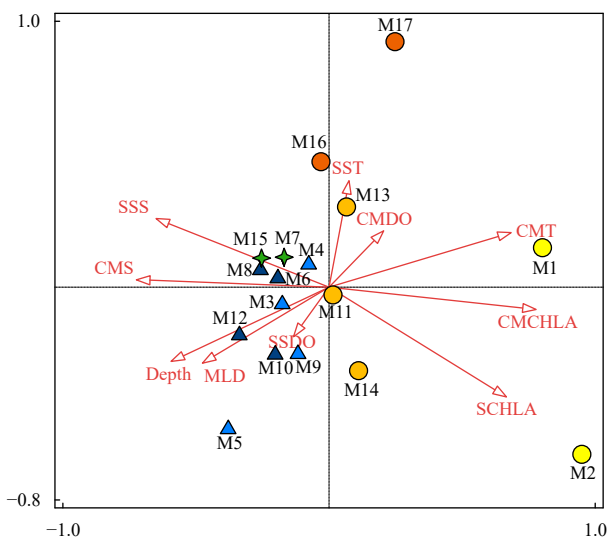


**Fig. 8.** Relationship between ten environmental variables and the mesozooplankton community by interactive-forward-selection RDA. Green stars indicate Group A; light and dark blue triangles indicate Groups B-1 and B-2, respectively; yellow, orange and light orange circles indicate Groups C-1, C-2 and C-3, respectively. MLD: mixed layer depth; SST: sea surface temperature; SSS: sea surface salinity; SDO: surface dissolved oxygen concentration; SCHLA: surface chlorophyll *a* concentration; CMT: column mean temperature; CMS: column mean salinity; CMDO: column mean dissolved oxygen concentration; CMCHLA: column mean chlorophyll *a* concentration.

**Table 5.** Results of interactive-forward-selection redundancy analyses

Environmental variables	Figure 8				Figure 10			
	Explains/%	pseudo-F	<i>p</i>	<i>p</i> (adj)	Explain/%	pseudo-F	<i>p</i>	<i>p</i> (adj)
CMCHLA	43.1	11.4	0.006	0.06	30.0	6.4	0.002	0.020
CMDO	12.7	4.0	0.030	0.3	5.2	1.4	0.232	1
CMT	12.6	5.2	0.008	0.08	6.6	1.8	0.148	1
CMS	6.6	3.2	0.030	0.3	10.5	2.5	0.018	0.162
SCHLA	2.6	1.3	0.260	1	5.6	1.6	0.158	1
SDO	2.4	1.2	0.282	1	1.5	0.4	0.822	1
SST	3.6	2.0	0.144	1	8.6	2.2	0.038	0.304
Depth	1.0	0.5	0.662	1	2.2	0.6	0.778	1
SSS	1.2	0.6	0.610	1	3.3	0.9	0.490	1
MLD	0.2	<0.1	0.980	1	5.1	1.6	0.186	1

Note: MLD: mixed layer depth; SST: sea surface temperature; SSS: sea surface salinity; SDO: surface dissolved oxygen concentration; SCHLA: surface chlorophyll *a* concentration; CMT: column mean temperature; CMS: column mean salinity; CMDO: column mean dissolved oxygen concentration; CMCHLA: column mean chlorophyll *a* concentration; adj: adjusted.



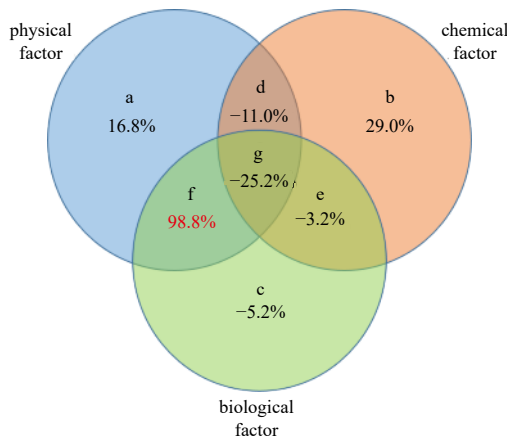


**Fig. 9.** Diagram of “Var-part-3groups-simple-effects-tested-FS” variation partition analysis. a, b, and c represent parts individually controlled by physical, chemical and biological factors, respectively; d represents the part controlled jointly by physical and chemical factors; e represents the part controlled jointly by chemical and biological factors; f represents the part controlled jointly by physical and biological factors; g represents the part controlled by physical, chemical and biological factors collectively. Values under the letters represent explained percentage. Physical factors include depth, mixed layer depth, sea surface temperature, sea surface salinity, column mean temperature, and column mean salinity; chemical factors include surface dissolved oxygen and column mean dissolved oxygen; and biological factors include surface chlorophyll *a* and column mean chlorophyll *a*.

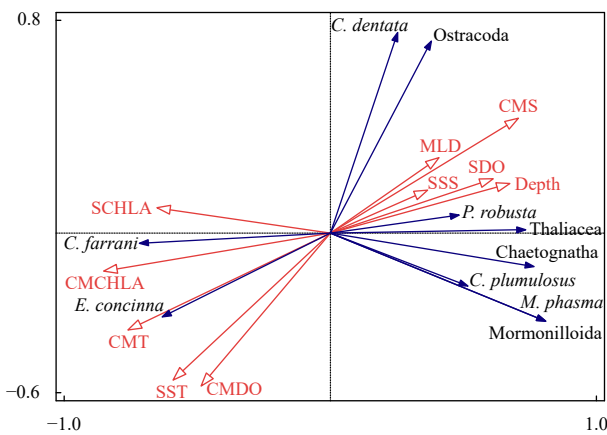


**Fig. 10.** Relationship between ten environmental variables and mesozooplankton taxa by interactive-forward-selection redundancy analysis. *C. farrani*: *Clausocalanus farrani*; *E. concinna*: *Euchaeta concinna*; *C. dentata*: *Cypridina dentata*; *P. robusta*: *Pleuromamma robusta*; *C. plumulosus*: *Calocalanus plumulosus*; *M. phasma*: *Mormonilla phasma*. MLD: mixed layer depth; SST: sea surface temperature; SSS: sea surface salinity; SDO: surface dissolved oxygen concentration; SCHLA: surface chlorophyll *a* concentration; CMT: column mean temperature; CMS: column mean salinity; CMDO: column mean dissolved oxygen concentration; CMCHLA: column mean chlorophyll *a* concentration.

differed among the coastal and oceanic stations (Fernandes and Ramaiah, 2014).

The total abundance in our study ranged from 337.5 ind./m<sup>3</sup> to 4 454.0 ind./m<sup>3</sup> (mean (1 916.7±1 192.9) ind./m<sup>3</sup>), which is lower

than those in the other Indian waters of western BOB coastal waters (4 473 ind./m<sup>3</sup> and 340–6 550 ind./m<sup>3</sup>) but much higher than those in other areas of the BOB (760.9 ind./m<sup>3</sup> and 277.0 ind./m<sup>3</sup>), as well as those in the western Pacific (206.6 ind./m<sup>3</sup> and 146.7 ind./m<sup>3</sup>) and the Arabian Sea (289.9 ind./m<sup>3</sup> and 371.3 ind./m<sup>3</sup>) (Table 6). The average dry biomass of mesozooplankton in our study ranged from 3.7 mg/m<sup>3</sup> to 30.7 mg/m<sup>3</sup> (mean (17.8±7.9) mg/m<sup>3</sup>; (6.10±2.72) mg/m<sup>3</sup> (in terms of C); 845.7 mg/m<sup>2</sup> (in terms of C), which is higher than those in the western BOB (777 mg/m<sup>2</sup>, in terms of C) and western tropical Pacific Ocean (4.9 mg/m<sup>3</sup>) but lower than those in areas of the BOB influenced by a cyclonic eddy (20.0 mg/m<sup>3</sup> in the central BOB and 35.9 mg/m<sup>3</sup> (in terms of C) in the southwestern BOB) and the Arabian Sea (14.7 mg/m<sup>3</sup> and 13.1 mg/m<sup>3</sup>, in terms of C) (Table 6). That is, the mesozooplankton abundance in this area was at a higher level in the Indo-Pacific Oceans, while the biomass was at a higher level in BOB and Pacific waters. This confirms that the Ayeyarwady Delta and Tanintharyi Coast are some of the most productive areas in the BOB, serving as an important spawning and nursery area for fisheries (Hossain et al., 2020). MLD is generally an important indicator of vertical mixing, which regulates the supply of deep nutrients to euphotic layers to change production in oligotrophic systems. However, the effect of MLD on mesozooplankton was not obvious in our study, probably since the area included a nearshore area with high productivity.

Seasonal variations in mesozooplankton biomass and abundance in the BOB vary from year to year due to eddies. Jyothibabu et al. (2008) found that the mesozooplankton biomass in the western BOB during summer and winter monsoons was higher than that during the spring intermonsoon above thermocline, and a cold-core eddy occurred during the winter sampling period in the study (Table 6). This variation is consistent with the simulation results of the large-scale spatiotemporal variation in the BOB based on existing observation data, which showed that the biomass from January–February was 2.60–2.70 mg/m<sup>3</sup> (in terms of C), followed by 2.49–2.51 mg/m<sup>3</sup> (in terms of C) from June–August and 1.58–1.70 mg/m<sup>3</sup> (in terms of C) from October–November (Hossain et al., 2020). However, Fernandes and Ramaiah (2019) found a higher biomass and abundance of mesozooplankton in the mixed layer during spring that was associated with cold-core eddies (Table 6). Therefore, annual studies are needed to understand the seasonal variation in zooplankton in the northern Andaman Sea.

Additionally, given that this area was dominated by a high percentage of picoplankton (64.1%), it could be inferred that microbial food webs were more dominant, where photosynthetic C was channeled to higher trophic levels through microzooplankton. Accordingly, the top 2 dominant mesozooplankton species were *Oncaea venusta* (relative abundance 9.9%–32.4%, mean 21.6%) and *Oithona* spp. (6.6%–22.3%, mean 12.6%), which were both omnivorous Cyclopoida and could effectively ambush and consume motile microzooplankton (Paffenhöfer, 1993). In conclusion, this area was an ecosystem of high productivity but still dominated by microbial food webs during winter.

#### 4.2 Spatial variations in the mesozooplankton community

The spatial distribution of the mesozooplankton community examined in this study reflects the existence of water mass exchange between the BOB and Andaman Sea. The mesozooplankton community similarity of some stations in the BOB and Andaman Sea exceeded 60% (e.g., between M7 and M15, and among M6, M12, M8, and M10; Fig. 6), suggesting that the Preparis Channel was an important water passage transporting marine

**Table 6.** Species number, abundance, and dry biomass of zooplankton in Indo-Pacific waters

Research area	Layer	Species number	Mesh size	Sampling time	Abundance/(ind.·m <sup>-3</sup> )	Dry biomass	Reference
Northern Andaman Sea off Myanmar	0–200 m (or bottom)	213	200 µm	February	1 916.7 (337.5–4 454.0)	17.8 mg/m <sup>3</sup> (3.7–30.7 mg/m <sup>3</sup> ) 6.1 mg/m <sup>3</sup> (in terms of C); 845.7 mg/m <sup>2</sup> (in terms of C)	this study
Other Indian waters	surface layer	–	200 µm	Spring	106.1–945.0	4.4–38.6 mg/m <sup>3</sup>	Jyothibabu et al. (2014)
off North coastal Andhra Pradesh	surface layer	112	200 µm	January, April, May, November	4 473.0	27.8 mg/m <sup>3</sup>	Rakesh et al. (2006)
off Rushikulya Estuary	0–bottom (<200 m)	93	120 µm	January–June	340.0–6 550.0	–	Mohanty et al. (2010)
Kodiakkara coastal waters	surface layer	121	158 µm	twelve months	–	–	Damotharan et al. (2010)
Open water western boundary currents in Pacific, in the subtropical North Pacific	0–200 m	–	160 µm	Winter	206.6 (35.1–456.8)	–	Dai et al. (2016)
Arabian Sea	0–200 m	259	200 µm	Summer	146.7	4.9 mg/m <sup>3</sup>	Yang et al. (2017)
southern BOB	0–200 m	187	505 µm	Spring	33.4	–	Li et al. (2017)
western BOB	0–bottom of thermocline	–	200 µm	Winter	–	777.0 mg/m <sup>2</sup> (in terms of C)	Jyothibabu et al. (2008)
southwestern BOB influenced by a cyclonic eddy	mixed layer	–	200 µm	Winter	760.9 (337.5–4 454.0)	35.9 mg/m <sup>3</sup> (in terms of C)	Jayalakshmi et al. (2015)
northern side of cyclonic eddy in central BOB	mixed layer	–	200 µm	Winter	277.0	20.0 mg/m <sup>3</sup> (in terms of C)	Sabu et al. (2015)
western Arabian Sea	0–150 m	–	333 µm	February	289.9	14.7 mg/m <sup>3</sup> (in terms of C)	Koppelman et al. (2003)
central Arabian Sea	0–150 m	–	333 µm	February	371.3	13.1 mg/m <sup>3</sup> (in terms of C)	Koppelman et al. (2003)
western BOB	0–bottom of thermocline	–	200 µm	Winter	–	777±433 mg/m <sup>2</sup> (in terms of C)	Jyothibabu et al. (2008)
				Spring	–	223±236 mg/m <sup>2</sup> (in terms of C)	Jyothibabu et al. (2008)
southwestern BOB				Summer	–	628±499 mg/m <sup>2</sup> (in terms of C)	Jyothibabu et al. (2008)
				Winter	70–4 288	8.9–35.9 mg/m <sup>3</sup> (in terms of C)	Jayalakshmi et al. (2015)
western BOB	mixed layer	–	200 µm	Spring	2–5 340	1.7–162.6 mg/m <sup>3</sup> (in terms of C)	Fernandes and Ramaiah (2019)
				Summer	25–4 621	1.3–31.0 mg/m <sup>3</sup> (in terms of C)	Fernandes and Ramaiah (2009)
				Autumn	100–2 482	2.4–53.6 mg/m <sup>3</sup> (in terms of C)	Fernandes and Ramaiah (2013)

Note: Conversion factors for deriving zooplankton carbon biomass from the displacement volume of zooplankton used were as follows: (1) 1 mL zooplankton = 75 mg dry weight; (2) 1 mg dry weight zooplankton = 0.342 mg carbon of zooplankton (Fernandes and Ramaiah, 2009). – represents no data.

species between the BOB and Andaman Sea. Water mass exchange between the Andaman Sea and BOB goes through three major channels: the northern channel (Preparis Channel) with a shallow depth of approximately 250 m, the middle channel including passages from south of the Andaman Islands to north of the Nicobar Islands with a maximum depth of approximately 800 m, and the southern channel (Great Channel) with a maximum depth of approximately 1 800 m (Chatterjee et al., 2017). The Preparis Channel is the channel with the largest net volume, with an annual mean transport value of  $0.64 \times 10^6 \text{ m}^3/\text{s}$  (Liao et al., 2020). Furthermore, transport in the Preparis Channel is relatively high in January and July, with net transport values of  $1.36 \times 10^6 \text{ m}^3/\text{s}$  and  $1.45 \times 10^6 \text{ m}^3/\text{s}$ , respectively, whereas in April and October, the water transport value is low and changes direction at 50 m depth (Liao et al., 2020). Therefore, substantial water exchange did occur during the sampling period, resulting in the mixing of mesozooplankton communities between the BOB and the Andaman Sea. However, the mesozooplankton communities in the shallow water on the continental shelf off the Ayeyarwady Delta, Gulf of Mottama and Tanintharyi Coast (Group C) were relatively isolated, likely due to the blocking effect of the Martaban Canyon (Fig. 1). The Martaban Canyon lies within a 120 km-wide bathymetric depression at the southern end of the Ayeyarwady Delta and Gulf of Mottama continental shelf (Rao et al., 2005), which incises the continental shelf (Ramaswamy et al., 2004), resulting in different oceanographic environments for the shelf and the deep Andaman Sea. The spatial patterns of zooplankton communities are linked to physical processes (ocean currents, eddies, jets, and diluted water), which affect zooplankton through effects on metabolic factors, primary productivity and predators (Fernández-Álamo and Färber-Lorda, 2006). The VPA showed that the interaction of physical (depth, MLD, SST, SSS, CMT and CMS) and biological (SCHLA and CMCHLA) factors determined the spatial variation of the mesozooplankton community (accounting for 98.8%) in our study. RDA results showed that the influences of CMCHLA and CMT were the most significant, accounting for 43.1% and 12.6%, respectively, and followed by CMDO (12.7%) and CMS (6.6%). Therefore, the physical processes affected the mesozooplankton community mainly through effects on primary productivity in this area.

Higher mesozooplankton biomass and abundance were detected along the Tanintharyi Coast and around the Ayeyarwady Delta, being approximately twice and six times as high as those of the transition zone and the open ocean, respectively. The spatial patterns of mesozooplankton biomass and abundance were the same as those of CMT and CMCHLA (Figs 5 and 7). Moreover, the high-value region of mesozooplankton biomass and abundance overlapped considerably with the low-value region of CMS (Figs 5 and 7). SST in the Andaman Sea was approximately  $3^\circ\text{C}$  higher than that in the BOB (Fig. 4). Liu et al. (2018) found that surface water was warmer in the Andaman Sea than in the BOB during the winter because of less heat loss, and the temperature difference was approximately  $1.5^\circ\text{C}$ . In addition, the northwestern part of the study area was covered by cold-core eddies during the sampling period (Fig. S1), which could also lower the SST in the BOB. However, the effects of offshore eddies on mesozooplankton communities were still uncertain, since an increase in SCHLA or CMCHLA was not detected (Figs 4 and 5). Based on the above, we proposed that less heat loss in the Andaman Sea and shallower coastal waters led to higher CMT along the Tanintharyi Coast and around the Ayeyarwady Delta. Additionally, the abundant mesozooplankton benefited from the freshwater influx. The influx of Ayeyarwady carrying richer nutrients caused

the lowest SSS and highest SCHLA levels near the Ayeyarwady Delta (especially at M2); the coastal freshwater influx and shallow water collectively caused the lowest CMS and highest CMCHLA levels along the Tanintharyi Coast and Ayeyarwady Delta. In summary, the spatial variation in mesozooplankton biomass and abundance in this area was directly controlled by CMCHLA, which was generated by CMT and CMS, which were simultaneously affected by heat loss, freshwater influx, eddies and depth.

The occurrence and abundance of species were related to hydrographic conditions and food availability (Fernández-Álamo and Färber-Lorda, 2006; Fernández De Puelles and Molinero, 2008; Fernandes, 2008; Srichandan et al., 2018). Accordingly, the relative abundances of warm water nearshore copepod (*Euchaeta concinna*) and copepod preferring phytoplankton (*Clausocalanus farrani*) were higher in Group C (Fig. 10). *Euchaeta concinna* is commonly found in the coastal waters of the western Pacific and northeastern Indian Ocean (Dur et al., 2007), mainly in ocean surface layers and warm waters (Jeong et al., 2011). *Clausocalanus farrani* was widely distributed in this area. However, the growth efficiency (mortality) of the copepodids was much higher (lower) when they fed on diatoms (phytoplankton) than when they fed on pellets (detritus) (Paffenhoefer and Knowles, 1979; Köster and Paffenhöfer, 2016), although they are omnivorous, nonselective feeders. Therefore, we observed that the distribution of *Clausocalanus farrani* was strongly positively correlated with chlorophyll *a* (both CMCHLA and SCHLA) (Fig. 10). Conversely, the relative abundance of mesobathypelagic copepods that could adapt well to  $\text{O}_2$ -deficient waters (*Calocalanus plumulosus*, *Pleuromamma robusta*, and *Mormonilla phasma*) (Irigoien and Harris, 2006; Ivanenko and Defaye, 2006; Cepeda et al., 2020) and of taxa preferring high saline environment (Ostracoda, Chaetognatha and Thaliacea) was higher in Groups A and B. The *Mormonilla phasma* (and the order Mormonilloida) and *Calocalanus plumulosus* were found only in the thermocline and below in the BOB (Fernandes and Ramaiah, 2009, 2013, 2019) and not at the surface layer at all (Fernandes and Ramaiah, 2014). *Pleuromamma robusta* was found to migrate vertically between the thermocline and the low oxygen zone in the BOB, Arabian Sea and eastern tropical Pacific (Fernández-Álamo and Färber-Lorda, 2006; Fernandes, 2008; Fernandes and Ramaiah, 2013, 2019). Ostracoda, Chaetognatha and Thaliacea are omnivorous, carnivorous and herbivorous, respectively, but they all prefer a salty environment (Jagadeesan et al., 2013; Li et al., 2010, 2017; Srichandan et al., 2018). On the other hand, Chaetognaths were considered to be a primary carnivore. Mills (1995) reviewed and concluded that numerous planktonic carnivore regions were characterized by low productivity, small phytoplankton and small copepods (Mills, 1995). In the present study, the proportion of pico-SCHLA was higher in Groups A and B (77.0% and 77.7%) than in Group C (59.6%) (Table 4), consistent with the characteristics of carnivores. Therefore, the mesozooplankton taxa spatial variation was controlled by CMCHLA, SST, and CMS together.

## 5 Conclusions

This paper reports the epipelagic mesozooplankton community and its relationship with environmental variables in the northern Andaman Sea off Myanmar in the winter. The abundances and species numbers in this area were both relatively rich in the Indo-Pacific waters, forming an important spawning and nursery area for fisheries. The top two dominant species, *Oncaea venusta* and *Oithona* spp., are both omnivorous Cyclopoida and

can effectively consume motile microzooplankton, suggesting that this ecosystem was still dominated by microbial food webs. In addition, this is an ecosystem with great spatial variation. Three mesozooplankton communities were identified: the open ocean, a transition zone and nearshore waters, which reflected the existence of water mass exchange between the BOB and Andaman Sea. Spatial variation was affected by physical processes mainly through their effects on primary productivity. The physical processes were affected simultaneously by heat loss differences, freshwater influx, eddies and depth. The great spatial variation in the mesozooplankton community may result from differences in the compositions of phytoplankton and microzooplankton, food web structure and energy transfer processes, which are worthy of further study.

#### Acknowledgements

We thank the cooperators in Myanmar and the captains and crews of the R/V *Xiangyanghong 6*, as well as the scientific parties of the cruise.

#### References

- Ashjian C J, Campbell R G, Gelfman C, et al. 2017. Mesozooplankton abundance and distribution in association with hydrography on Hanna Shoal, NE Chukchi Sea, during August 2012 and 2013. *Deep-Sea Research Part II: Topical Studies in Oceanography*, 144: 21–36, doi: [10.1016/j.dsr2.2017.08.012](https://doi.org/10.1016/j.dsr2.2017.08.012)
- Cepeda G D, Viñas M D, Molinari G N, et al. 2020. The impact of Río de la Plata plume favors the small-sized copepods during summer. *Estuarine, Coastal and Shelf Science*, 245: 107000
- Chatterjee A, Shankar D, McCreary J P, et al. 2017. Dynamics of Andaman Sea circulation and its role in connecting the equatorial Indian Ocean to the Bay of Bengal. *Journal of Geophysical Research: Oceans*, 122(4): 3200–3218, doi: [10.1002/2016JC012300](https://doi.org/10.1002/2016JC012300)
- Cornils A, Schnack-Schiel S B, Böer M, et al. 2006. Feeding of Clausocalanids (Calanoida, Copepoda) on naturally occurring particles in the northern Gulf of Aqaba (Red Sea). *Marine Biology*, 151(4): 1261–1274
- Dai Luping, Li Chaolun, Yang Guang, et al. 2016. Zooplankton abundance, biovolume and size spectra at western boundary currents in the subtropical North Pacific during winter 2012. *Journal of Marine Systems*, 155: 73–83, doi: [10.1016/j.jmarsys.2015.11.004](https://doi.org/10.1016/j.jmarsys.2015.11.004)
- Damotharan P, Perumal N V, Arumugam M, et al. 2010. Studies on zooplankton ecology from Kodiakkarai (point calimere) coastal waters (south east coast of India). *Research Journal of Biological Sciences*, 5(2): 187–198, doi: [10.3923/rjbsci.2010.187.198](https://doi.org/10.3923/rjbsci.2010.187.198)
- Domínguez R, Garrido S, Santos A M P, et al. 2017. Spatial patterns of mesozooplankton communities in the northwestern Iberian shelf during autumn shaped by key environmental factors. *Estuarine, Coastal and Shelf Science*, 198: 257–268
- Dur G, Hwang J S, Souissi S, et al. 2007. An overview of the influence of hydrodynamics on the spatial and temporal patterns of calanoid copepod communities around Taiwan. *Journal of Plankton Research*, 29(S1): i97–i116
- Fernandes V. 2008. The effect of semi-permanent eddies on the distribution of mesozooplankton in the central Bay of Bengal. *Journal of Marine Research*, 66(4): 465–488, doi: [10.1357/002224008787157430](https://doi.org/10.1357/002224008787157430)
- Fernandes V, Ramaiah N. 2009. Mesozooplankton community in the Bay of Bengal (India): spatial variability during the summer monsoon. *Aquatic Ecology*, 43(4): 951–963, doi: [10.1007/s10452-008-9209-4](https://doi.org/10.1007/s10452-008-9209-4)
- Fernandes V, Ramaiah N. 2013. Mesozooplankton community structure in the upper 1,000 m along the western Bay of Bengal during the 2002 fall intermonsoon. *Zoological Studies*, 52(1): 31, doi: [10.1186/1810-522X-52-31](https://doi.org/10.1186/1810-522X-52-31)
- Fernandes V, Ramaiah N. 2014. Distributional characteristics of surface-layer mesozooplankton in the Bay of Bengal during the 2005 winter monsoon. *Indian Journal of Geo-Marine Sciences*, 43(1): 176–188
- Fernandes V, Ramaiah N. 2019. Spatial structuring of zooplankton communities through partitioning of habitat and resources in the Bay of Bengal during spring intermonsoon. *Turkish Journal of Zoology*, 43(1): 68–93, doi: [10.3906/zoo-1805-6](https://doi.org/10.3906/zoo-1805-6)
- Fernández-Álamo M A, Färber-Lorda J. 2006. Zooplankton and the oceanography of the eastern tropical Pacific: A review. *Progress in Oceanography*, 69(2–4): 318–359
- Fernández De Puellas M L, Molinero J C. 2008. Decadal changes in hydrographic and ecological time-series in the Balearic Sea (western Mediterranean), identifying links between climate and zooplankton. *ICES Journal of Marine Science*, 65(3): 311–317, doi: [10.1093/icesjms/fsn017](https://doi.org/10.1093/icesjms/fsn017)
- Gomes H R, Goes J I, Saino T. 2000. Influence of physical processes and freshwater discharge on the seasonality of phytoplankton regime in the Bay of Bengal. *Continental Shelf Research*, 20(3): 313–330, doi: [10.1016/S0278-4343\(99\)00072-2](https://doi.org/10.1016/S0278-4343(99)00072-2)
- Hossain M S, Sarker S, Sharifuzzaman S M, et al. 2020. Primary productivity connects hilsa fishery in the Bay of Bengal. *Scientific Reports*, 10(1): 5659, doi: [10.1038/s41598-020-62616-5](https://doi.org/10.1038/s41598-020-62616-5)
- Irigoiien X, Harris R P. 2006. Comparative population structure, abundance and vertical distribution of six copepod species in the North Atlantic: Evidence for intraguild predation?. *Marine Biology Research*, 2(4): 276–290
- Ittekkot V, Nair R R, Honjo S, et al. 1991. Enhanced particle fluxes in Bay of Bengal induced by injection of fresh water. *Nature*, 351(6325): 385–387, doi: [10.1038/351385a0](https://doi.org/10.1038/351385a0)
- Ivanenko V N, Defaye D. 2006. Planktonic deep-water copepods of the family Mormonillidae Giesbrecht, 1893 from the East Pacific Rise (13°N), the Northeastern Atlantic, and near the North Pole (Copepoda, Mormonilloida). *Crustaceana*, 79(6): 707–726, doi: [10.1163/156854006778026861](https://doi.org/10.1163/156854006778026861)
- Jagadeesan L, Jyothibabu R, Anjusha A, et al. 2013. Ocean currents structuring the mesozooplankton in the Gulf of Mannar and the Palk Bay, southeast coast of India. *Progress in Oceanography*, 110: 27–48, doi: [10.1016/j.pocean.2012.12.002](https://doi.org/10.1016/j.pocean.2012.12.002)
- Jagadeesan L, Jyothibabu R, Arunpandi N, et al. 2017. Dominance of coastal upwelling over Mud Bank in shaping the mesozooplankton along the southwest coast of India during the Southwest Monsoon. *Progress in Oceanography*, 156: 252–275, doi: [10.1016/j.pocean.2017.07.004](https://doi.org/10.1016/j.pocean.2017.07.004)
- Jayalakshmi K J, Sabu P, Devi C R A, et al. 2015. Response of micro- and mesozooplankton in the southwestern Bay of Bengal to a cyclonic eddy during the winter monsoon, 2005. *Environmental Monitoring and Assessment*, 187(7): 473, doi: [10.1007/s10661-015-4609-0](https://doi.org/10.1007/s10661-015-4609-0)
- Jeong M K, Suh H L, Soh H Y. 2011. Taxonomy and zoogeography of euchaetid copepods (Calanoida, Clausocalanoidea) from Korean waters, with notes on their female genital structure. *Ocean Science Journal*, 46(2): 117–132, doi: [10.1007/s12601-011-0011-1](https://doi.org/10.1007/s12601-011-0011-1)
- Jyothibabu R, Madhu N V, Maheswaran P A, et al. 2008. Seasonal variation of microzooplankton (20–200 µm) and its possible implications on the vertical carbon flux in the western Bay of Bengal. *Continental Shelf Research*, 28(6): 737–755, doi: [10.1016/j.csr.2007.12.011](https://doi.org/10.1016/j.csr.2007.12.011)
- Jyothibabu R, Win N N, Shenoy D M, et al. 2014. Interplay of diverse environmental settings and their influence on the plankton community off Myanmar during the Spring Intermonsoon. *Journal of Marine Systems*, 139: 446–459, doi: [10.1016/j.jmarsys.2014.08.003](https://doi.org/10.1016/j.jmarsys.2014.08.003)
- Koppelman R, Fabian H, Weikert H. 2003. Temporal variability of deep-sea zooplankton in the Arabian Sea. *Marine Biology*, 142(5): 959–970, doi: [10.1007/s00227-002-0999-y](https://doi.org/10.1007/s00227-002-0999-y)
- Köster M, Paffenhöfer G A. 2016. How efficiently can doliolids (Tunicata, Thaliacea) utilize phytoplankton and their own fecal pellets?. *Journal of Plankton Research*, 39(2): 305–315
- Li Kaizhi, Yin Jianqiang, Huang Liangmin, et al. 2010. Advances on classification and ecology of pelagic tunicates. *Acta Ecologica Sinica (in Chinese)*, 30(1): 174–185

- Li Kaizhi, Yin Jianqiang, Huang Liangmin, et al. 2017. A comparison of the zooplankton community in the Bay of Bengal and South China Sea during April–May, 2010. *Journal of Ocean University of China*, 16(6): 1206–1212, doi: [10.1007/s11802-017-3229-4](https://doi.org/10.1007/s11802-017-3229-4)
- Liao Jiawen, Peng Shiqiu, Wen Xixi. 2020. On the heat budget and water mass exchange in the Andaman Sea. *Acta Oceanologica Sinica*, 39(7): 32–41, doi: [10.1007/s13131-019-1627-8](https://doi.org/10.1007/s13131-019-1627-8)
- Liu Yanliang, Li Kuiping, Ning Chunlin, et al. 2018. Observed seasonal variations of the upper ocean structure and air-sea interactions in the Andaman Sea. *Journal of Geophysical Research: Oceans*, 123(2): 922–938, doi: [10.1002/2017JC013367](https://doi.org/10.1002/2017JC013367)
- Madhu N V, Jyothibabu R, Maheswaran P A, et al. 2006. Lack of seasonality in phytoplankton standing stock (chlorophyll *a*) and production in the western Bay of Bengal. *Continental Shelf Research*, 26(16): 1868–1883, doi: [10.1016/j.csr.2006.06.004](https://doi.org/10.1016/j.csr.2006.06.004)
- Madhupratap M, Gauns M, Ramaiah N, et al. 2003. Biogeochemistry of the Bay of Bengal: physical, chemical and primary productivity characteristics of the central and western Bay of Bengal during summer monsoon 2001. *Deep-Sea Research Part II: Topical Studies in Oceanography*, 50(5): 881–896, doi: [10.1016/S0967-0645\(02\)00611-2](https://doi.org/10.1016/S0967-0645(02)00611-2)
- McCreary J P, Kundu P K, Molinari R L. 1993. A numerical investigation of dynamics, thermodynamics and mixed-layer processes in the Indian Ocean. *Progress in Oceanography*, 31(3): 181–244, doi: [10.1016/0079-6611\(93\)90002-U](https://doi.org/10.1016/0079-6611(93)90002-U)
- Mills C E. 1995. Medusae, siphonophores, and ctenophores as planktivorous predators in changing global ecosystems. *ICES Journal of Marine Science*, 52(3–4): 575–581
- Mohanty A K, Sahu G, Singhsamanta B, et al. 2010. Zooplankton diversity in the nearshore waters of Bay of Bengal, off Rushikulya Estuary. *The IUP Journal of Environmental Sciences*, 4(2): 61–85
- Nuncio M, Kumar S P. 2012. Life cycle of eddies along the western boundary of the Bay of Bengal and their implications. *Journal of Marine Systems*, 94: 9–17, doi: [10.1016/j.jmarsys.2011.10.002](https://doi.org/10.1016/j.jmarsys.2011.10.002)
- Paffenhofer G A, Knowles S C. 1979. Ecological implications of fecal pellet size, production and consumption by copepods. *Journal of Marine Research*, 37: 35–49
- Paffenhöfer G A. 1993. On the ecology of marine cyclopoid copepods (Crustacea, Copepoda). *Journal of Plankton Research*, 15(1): 37–55, doi: [10.1093/plankt/15.1.37](https://doi.org/10.1093/plankt/15.1.37)
- Prasanna Kumar S, Muraleedharan P M, Prasad T G, et al. 2002. Why is the Bay of Bengal less productive during summer monsoon compared to the Arabian Sea?. *Geophysical Research Letters*, 29(24): 2235
- Prasanna Kumar S, Narvekar J, Nuncio M, et al. 2010. Is the biological productivity in the Bay of Bengal light limited?. *Current Science*, 98(10): 1331–1339
- Prasanna Kumar S, Nuncio M, Narvekar J, et al. 2004. Are eddies nature's trigger to enhance biological productivity in the Bay of Bengal?. *Geophysical Research Letters*, 31(7): L07309
- Rakhesh M, Raman A V, Sudarsan D. 2006. Discriminating zooplankton assemblages in neritic and oceanic waters: a case for the northeast coast of India, Bay of Bengal. *Marine Environmental Research*, 61(1): 93–109, doi: [10.1016/j.marenvres.2005.06.002](https://doi.org/10.1016/j.marenvres.2005.06.002)
- Ramaswamy V, Gaye B, Shirodkar P V, et al. 2008. Distribution and sources of organic carbon, nitrogen and their isotopic signatures in sediments from the Ayeyarwady (Irrawaddy) continental shelf, northern Andaman Sea. *Marine Chemistry*, 111(3–4): 137–150
- Ramaswamy V, Rao P S, Rao K H, et al. 2004. Tidal influence on suspended sediment distribution and dispersal in the northern Andaman Sea and Gulf of Martaban. *Marine Geology*, 208(1): 33–42, doi: [10.1016/j.margeo.2004.04.019](https://doi.org/10.1016/j.margeo.2004.04.019)
- Rao P S, Ramaswamy V, Thwin S. 2005. Sediment texture, distribution and transport on the Ayeyarwady continental shelf, Andaman Sea. *Marine Geology*, 216(4): 239–247, doi: [10.1016/j.margeo.2005.02.016](https://doi.org/10.1016/j.margeo.2005.02.016)
- Rodolfo K S. 1969. Sediments of the Andaman Basin, northeastern Indian Ocean. *Marine Geology*, 7(5): 371–402, doi: [10.1016/0025-3227\(69\)90014-0](https://doi.org/10.1016/0025-3227(69)90014-0)
- Sabu P, Devi C R A, Lathika C T, et al. 2015. Characteristics of a cyclonic eddy and its influence on mesozooplankton community in the northern Bay of Bengal during early winter monsoon. *Environmental Monitoring and Assessment*, 187(6): 330, doi: [10.1007/s10661-015-4571-x](https://doi.org/10.1007/s10661-015-4571-x)
- Schott F A, McCreary J P. 2001. The monsoon circulation of the Indian Ocean. *Progress in Oceanography*, 51(1): 1–123, doi: [10.1016/S0079-6611\(01\)00083-0](https://doi.org/10.1016/S0079-6611(01)00083-0)
- Shankar D, Vinayachandran P N, Unnikrishnan A S. 2002. The monsoon currents in the north Indian Ocean. *Progress in Oceanography*, 52(1): 63–120, doi: [10.1016/S0079-6611\(02\)00024-1](https://doi.org/10.1016/S0079-6611(02)00024-1)
- Skjoldal H R, Wiebe P H, Postel L, et al. 2013. Intercomparison of zooplankton (net) sampling systems: results from the ICES/GLOBEC sea-going workshop. *Progress in Oceanography*, 108: 1–42, doi: [10.1016/j.pocean.2012.10.006](https://doi.org/10.1016/j.pocean.2012.10.006)
- Šmilauer P, Lepš J. 2014. *Multivariate analysis of ecological data using Canoco 5*, second edition. Cambridge, UK: Cambridge University Press, 362
- Srichandan S, Baliarsingh S K, Prakash S, et al. 2018. Zooplankton research in Indian seas: a review. *Journal of Ocean University of China*, 17(5): 1149–1158, doi: [10.1007/s11802-018-3463-4](https://doi.org/10.1007/s11802-018-3463-4)
- Steinberg D K, Lomas M W, Cope J S. 2012. Long-term increase in mesozooplankton biomass in the Sargasso Sea: linkage to climate and implications for food web dynamics and biogeochemical cycling. *Global Biogeochemical Cycles*, 26(1): GB1004
- Subramanian V. 1993. Sediment load of Indian Rivers. *Current Science*, 64(11–12): 928–930
- Yang Guang, Li Chaolun, Wang Yanqing, et al. 2017. Spatial variation of the zooplankton community in the western tropical Pacific Ocean during the summer of 2014. *Continental Shelf Research*, 135: 14–22, doi: [10.1016/j.csr.2017.01.009](https://doi.org/10.1016/j.csr.2017.01.009)
- Yuan L L, Pollard A I. 2018. Changes in the relationship between zooplankton and phytoplankton biomasses across a eutrophication gradient. *Limnology and Oceanography*, 63(6): 2493–2507, doi: [10.1002/lno.10955](https://doi.org/10.1002/lno.10955)

## Supplementary information:

**Fig. S1.** The sea-level anomalies (SLAs, m) with current vectors (m/s) during the sampling period.

**Table S1.** Information on mesozooplankton sample collection.

**Table S2.** Abbreviations, explanations, and sources of the environmental variables used in this study.

**Table S3.** Results of “Var-part-3groups-simple-effects-tested-FS” VPA.

**Table S4.** Correlation coefficients between the biomass and abundance of mesozooplankton and environmental variables in Spearman correlation analyses.

The supplementary information is available online at <https://doi.org/10.1007/s13131-022-2090-5> and <http://www.aosocean.com/>. The supplementary information is published as submitted, without typesetting or editing. The responsibility for scientific accuracy and content remains entirely with the authors.